April 2019

Transcriptional Regulation of Non-Coding RNAs by Retinoblastoma Tumor Suppressor Protein

Hammad M. Sadiq
Worcester Polytechnic Institute

Follow this and additional works at: https://digitalcommons.wpi.edu/mqp-all

Transcriptional Regulation of Non-Coding RNAs

by Retinoblastoma Tumor Suppressor Protein

_____

A Major Qualifying Project Report

Submitted to

WORCESTER POLYTECHNIC INSTITUTE,

In Partial Fulfillment of the Requirements for the Degree of Bachelor of Science

In

Biology & Biotechnology

_____

Authored By:

Hammad Sadiq

April 25th, 2019

Approved by:

Amity L. Manning, PhD

Biology and Biotechnology

MQP Project Advisor

Abstract

Recent advances in whole transcriptome sequencing have revealed that the majority of the genome is transcribed but only 1% of transcripts are coded for protein biosynthesis. This remaining 'junk DNA' includes non-coding RNA species (ncRNA), which have been implicated in modulating tumorigenesis as well as tumor suppression if they are misexpressed. Recent experiments indicate that loss of the Retinoblastoma tumor suppressor protein (pRB), a transcriptional co-regulator, alters the expression of both coding and non-coding transcripts. This project seeks to understand if misexpression of these ncRNAs plays a role in the pleiotropic effects of pRB loss in cancer.

Acknowledgements

Firstly, I want to thank my project advisor Amity Manning for supporting me and guiding me through this project. In my time in lab, and especially during this MQP, I have gained a whole new appreciation for scientific research under her guidance. This feeling was bolstered by her constant support about completing a more exploratory project. I also want to thank the other members of the lab including, Nicole Hermance, Conor Herilhy, Elizabeth Crowley, Dayna Mercadante, Luis Gregory Gutierrez and Sabine Hahn for their constant help and enthusiasm throughout my time at the lab.

Table of Contents

List of Tables

List of Figures

Introduction & Background

Overview of Retinoblastoma Protein (pRB) Pathway and Human Cancers

Figure 1: pRB is a central transcriptional regulator of cell proliferation and cell cycle progression. Regulation of the cell cycle G1/S transition by cyclin D1, CDK4 and p16. RB, retinoblastoma protein, CDK4/6, cyclin-dependent kinase 4/6.Textbook model of pRB pathway. When pRB is bound to E2F transcription is repressed. Once pRB is phosphorylated, E2F is free to bind to genomic DNA to allow for the transcription of a given gene.
Retrieved from: Peurala, E., Koivunen, P., Haapasaari, K., Bloigu, R., & Jukkola-Vuorinen, A. (2013). The prognostic significance and value of cyclin D1, CDK4 and p16 in human breast cancer. *Breast Cancer Research: BCR*, *15*(1), R5–R5..

The Retinoblastoma protein (pRB) is a central transcriptional regulator of cell proliferation and cell cycle progression. pRB was first identified as a gene that was associated with pediatric eye tumorigenesis, or Retinoblastoma over 25 years ago (Nevins, 2001; Dick & Rubin, 2013; Elchuri et al., 2018). Additionally, a great body of research has implicated deregulation of pRB's function in uncontrolled cell cycle progression, as well as tumorigenesis of many

human cancers (Dyson, 2016; Nevins, 2001). Thus, it is important to consider how pRB mediates mitosis. pRB's function can be categorized as a negative regulator of the cell cycle (Dick & Rubin, 2013). The function and regulation of pRB is more complex however, as it involves the activity of numerous stimuli which act as pRB function regulators (Dick & Rubin, 2013; Peurala et al., 2013). Normally or in the absence of extracellular signals pRB is bound to E2F (as seen in Figure 1) preventing the transcription of genes needed for DNA replication; this inhibition of E2F transcription is why pRB is often referred as a tumor suppressor as this action prevents unscheduled entry of cells into the cell cycle by inducing G1 phase cell-cycle arrest (Dick & Rubin, 2013; Knudsen & Knudsen, 2008). When appropriate mitogenic conditions are met such

as growth stimulation, pRB is phosphorylated through the activity of cyclin D1 and its partner

CDK4/6 kinases (Dick & Rubin, 2013; Nevins, 2001; Knudsen & Knudsen, 2008; Weinberg, 1995). At this point, p16 referred to as p16^{INK4A}, an inhibitor of CDKs aids in maintaining pRB's phosphorylated state by inhibiting the activity of CDK4/6 (Peurala et al., 2013). Phosphorylated pRB detaches from the E2F allowing for gene transcription and cell cycle progression.

Many cancers devise mechanisms to impair pRB function by mutating the RB gene or altering the expression of RB

Cancer type	Loss of p16^{INK4A}	Overexpression of cyclin D1^{*-}	Loss of RB	RB activity (indirect)
SCLC	<10% ND	<10% ND	>90% ND	Not assessed
NSCLC	40−60% indeterminate	40−60% indeterminate	10−20% indeterminate	Poor outcome
Bladder	20−40% poor outcome	20−80% favourable outcome	30−70% poor outcome	Not assessed
Prostate	10−40% indeterminate	0−35% indeterminate	30−60% indeterminate	Poor outcome
Melanoma	40−60% poor outcome	30−60% no influence	10−40% no influence	Not assessed
Pancreas	40−70% poor outcome	50−70% indeterminate	<5% ND	Not assessed
Colorectal	30−60% no influence	40−60% no influence	0−20% no influence	Not assessed
Liver	30−70% indeterminate	20−40% indeterminate	20−40% indeterminate	Poor outcome
Breast	20−40% indeterminate	30−70% favourable outcome (ER-positive)	10−30% indeterminate (ER-negative)	Poor outcome

Figure 2: pRB pathway heterogeneity in primary tumors. Consensus percentages reflective of numerous studies. Not assessed or indeterminate refers to research where a consensus has yet to be reached. ND refers to non-determined. SCLC and NSCLC refer to small and non-small cell lung cancer.

Adapted from: Knudsen, Erik S., and Karen E. Knudsen. "Tailoring to RB: tumour suppressor status and therapeutic response." Nature Reviews Cancer, vol. 8, no. 9, 2008, p. 714+.

regulators (Figure 1) such as cyclin D, CDK 4 and 6 and p16 which inhibits them (Dick & Rubin, 2013). One can assume that a disruption in this pathway may result tumorigeneses (Weinberg, 1995). These species are all involved in what is referred to as the p16-cyclin-CDK4/6-pRB pathway, which is compromised in many human cancers such as breast cancer (Peurala et al., 2013; Weinberg, 1995; Dyson, 2016; Nevin 2001). As illustrated in Figure 2, there is variation in how the pRB pathway is altered in a given the specific cancer phenotype. For

example, the researchers Peurala et al. (2013) found that overexpression of cyclin D1 is correlated with a lower grade of tumor and thus a more favorable prognosis.

In other cancers such as small lung cancers, retinoblastomas and bladder cancers pRB is known to be lost (Horowitz et al., 1990; Weinberg, 1995). p16 loss is another common feature in lung cancers has been studied as a biomarker for this cancer type (Weinberg, 1995; Tong et al., 2011). This is in part, due to normally high levels of p16 found via immunohistochemistry approaches in lung tissue which reach near undetectable levels in lung carcinomas (Tong et al., 2011).

The various changes that have been discussed all affect the function of pRB and as a direct consequence, E2F is free to cause an uncontrolled proliferation of cellular proliferation, which is one of the many factors that results in tumorigenesis (Nevin, 2001). Thus, pRB plays a fundamental role in preventing oncogenic growth (Elchuri et al., 2018). Prior research, however, has shown that the loss or inactivation of pRB has more complex effects in response to cancer therapeutics specifically and may be a metric or avenue for the development of therapies (Knudsen & Knudsen, 2008).

Additionally, recent microarray data as well as the advent of unbiased RNA sequencing (which measures all the RNA in a cell) has aided in whole transcriptome analysis and identified several genomic aberrations Retinoblastoma tumors such as non-coding RNAs, pseudogenes as well as RNA fusions which are characterized by altered RNA processing events (Elchuri et al., 2018).

Overview of Non-coding RNAs

As potential altered transcripts in response to pRB loss for example, is important to understand and their significance as it pertains to cancer. Recent advances in transcriptome

sequencing has revealed that ~70-90% of the transcripts are expressed, but only 1% is responsible for coding proteins. This genomic dark matter is transcribed and yet it's functions remain uncertain (Lee, 2012; Romano et al., 2017). What was originally thought as 'junk-DNA,' has now been shown to include noncoding species such as pseudogenes, intronic sequences, repeat sequences and most prominently noncoding RNA elements (Romano et al., 2017). These have been sorted by size, with transcripts longer than 200 nucleotides being referred to long non-coding RNAs (lncRNAs) and shorter transcripts are referred to as short-interfering and microRNAs (siRNAs & miRNAs) (Zhuang et al., 2016; Romano et al., 2017). While ncRNAs such as tRNAs and rRNAs function has been clearly categorized, recent research has focused on the regulatory roles of ncRNA (Romano et al., 2017). Many noncoding sequences of RNA play regulatory roles in various contexts and can influence the epigenetic, transcriptional, and post-transcriptional regulation of genes (Kruer et al, 2016; Romano et al., 2017). As illustrated in Figure 3, these functional outcomes are a result of interactions with: 1) DNA, as lncRNA can alter chromatin structure and thus affect gene expression, 2) protein, as lncRNA can form protein-protein complexes that hinder or promote protein-protein interactions and 3) RNA, as ncRNA can affect mRNA decay and regulate expression of certain mRNA species (Schmitt & Chang, 2016; Romano et al., 2017). ncRNAs have also been implicated in modulating tumorigenesis and tumor suppression (Schmitt & Chang, 2016; Huarte, 2015; Wang et al., 2016). Misregulation of ncRNAs is associated with a poor prognosis and this dysregulated expression can be used as a biomarker for disease progression (Romano et al., 2017; Schmitt & Chang, 2016; Huarte, 2015). Certain ncRNAs are involved in tumor suppression circuits involving pRB, such as the lncRNA MEG3 (Kruer et al, 2016; Schmitt & Chang).

Non-coding RNAs and pRB

In some human cancers such as Retinoblastoma, the loss of pRB is one of the nascent events that leads to tumorigenesis (Elchuri et al., 2018; Nevin 2001). And as discussed earlier, it is known pRB acts as a transcriptional regulator of the E2F family of transcription factors which are involved in the transcription of certain genes, but very little is understood about how this complex influences the expression of non-coding RNAs (Nevins, 2001; Dick & Rubin, 2013; Elchuri et al., 2018). Some labs armed with microarray data have attempted to understand the transcriptional changes in RB deficient sample and normal retinal pigment control cells (Zhang et al., 2012). There is also evidence of more direct influence of E2F binding in genomic loci of some non-coding RNAs which was determined via chromatin immunoprecipitation or ChIP experiments (Xu et al., 2007). These initial experiments provide hints at the potential of E2F and RB as potential transcriptional regulators of non-coding RNAs.

Recently the Manning lab has produced preliminary some RNA sequencing datasets (as seen in Figure 4). These data were produced in non-transformed human epithelial cell line known as Retinal pigment Epithelium (RPE-1) where pRB was knocked-out (KO) via siRNA approaches. This RNA sequencing produced over 4000 misregulated transcripts which include protein-coding, non-coding and pseudogenes. Of these about 200 ncRNA are differentially and significantly upregulated in RPE-1 following pRB K), and ~50 non-coding RNA were very significantly upregulated.
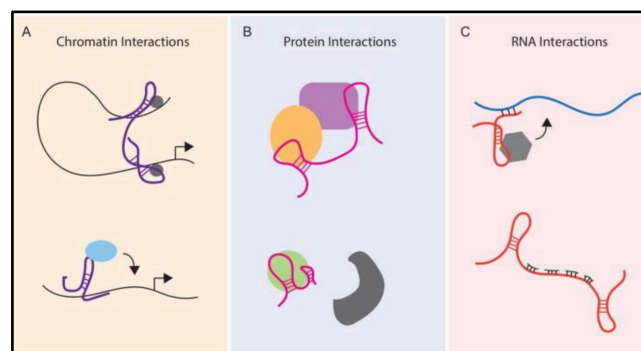

Figure 3: ncRNA interactions with macromolecules.

ncRNA interactions are dependent on interactions with macromolecule interactions.

Retrieved from: Schmitt, Adam M., and Howard Y. Chang (2016). "Long Noncoding RNAs in Cancer Pathways." Cancer cell 29.4 (2016): 452–463. PMC. Web. 13 Oct. 2018.

Some of these upregulated non-coding RNAs have intriguing roles as it pertains to tumorigenesis (purple dots in Figure 4). One such ncRNA is long intergenic non-coding RNA or LINC00342 which has been implicated as a potential biomarker for patients who have non-small lung cancer or NSLSC, the most prevalent type of lung cancer and involved in the most deaths (Tang et al., 2019). The researchers Tang et al. (2019) studied serum, and tumor tissue samples of NSCLC patients and found evidence for
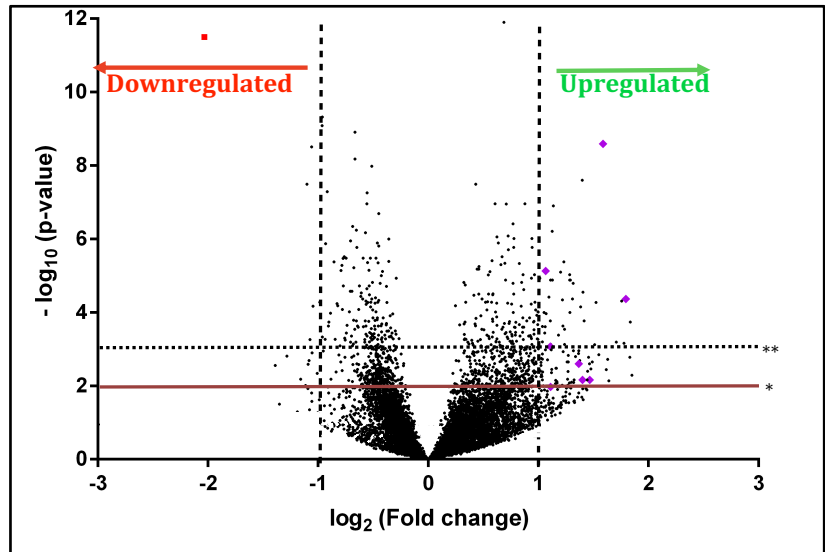
Figure 4: A volcano plot representation of differentially expressed coding and non-coding transcripts following knockout of pRB. The log Fold Change of the gene expression levels observed following siRNA-based knockout of pRB is reported on the X axis, while the –log 10 of the p-value of the statistical test of differential expression (t-test) is shown on the Y axis. The RNAseq presented 3906 genes that were misregulated following KO of pRB. And it produced 200 coding, noncoding and pseudogenes that were significantly upregulated (p-value <0.01) and had fold change value >1. Of those 200, a total of 50 noncoding genes were significantly upregulated (p-value <0.01) and had log fold changes >1. Additionally, 30 ncRNA were significantly upregulated (p-value <0.001) and had log fold change values >1. The horizontal red line represents a statistical difference threshold of 0.01 for the p-value. The dashed horizontal line represents a statistical difference threshold of 0.001 for the p-value. Non-coding RNAs that had p-values were greater than the threshold of 0.001 were biologically misregulated and were of interest were labeled with purple dots.

LINC00342 as a biomarker for this cancer, as its higher expression of it is associated with a poor prognosis. Interestingly they also found that this overexpression promotes uncontrolled cell proliferation, a phenotype shared by many human cancers, by inhibiting p53 and PTEN which are proteins involved in cellular proliferation (Tang et al., 2019; Dick & Rubin, 2013). Other ncRNAs that were identified in this screen include brain derived neurotrophic factor antisense or BDNF-AS which had striking functional relevance to cancer (de Farias et al, 2012; Shang et al.,

Figure 5: Effect of BDNF-AS upregulation on RB cell proliferation and migration. A transwell migration assay performed on WERI-Rb-1 cells. Migrating RB cells in lo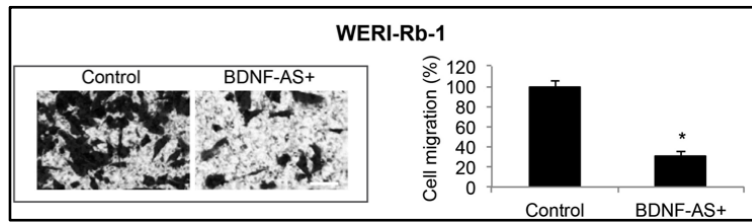wer chambers were visualized through staining of crystal violet (left, scale bar: 20 μM). Relative migration capability was compared between Control RB cells and cells with BDNF-AS upregulation (right, *P < 0.05).

Retrieved from: Shang, W., Yang, Y., Zhang, J., & Wu, Q. (2018). Long noncoding RNA BDNF-AS is a potential biomarker and regulates cancer development in human retinoblastoma. Biochemical and Biophysical Research Communications, 497(4), 1142–1148.

2018). Previous research has shown that BDNF-AS is a inverse regulator of the coding transcript BDNF, thus has profound effects on neuronal development (Shang et al., 2018). The researchers de Farias (2012) found that when colorectal tumor samples were exposed to anti-cancer drugs that affect proliferation by blocking growth factors, was compromised following the addition of BDNF-AS. This implies that BDNF-AS has some role in the proliferation of cells and tumorigenesis. Recently the efficacy of BDNF-AS as a biomarker for human cancer was assessed, and in Retinoblastoma tumor (RB) samples as well as RB cell lines a high level of BDNF-AS were present (Shang et al., 2018). Most strikingly, when BDNF-AS was overexpressed in RB tumor cell line, these cells exhibited was lower motility and proliferation, than compared to control RB tumor cells in transwell migration assay as illustrated in Figure 5.

Objective & Hypothesis

Previous research has shown that certain ncRNAs are dysregulated during tumorigenesis. This project will employ RNA sequencing data that the Manning Lab generated using a non-transformed human epithelial cell line known as Retinal pigment Epithelium (RPE-1) and cells that are genetically identical but have been depleted of the pRB protein via siRNA. The aim is to explore which ncRNAs are misexpressed and are either upregulated or downregulated in

response to pRB loss. Additionally, the functional relevance of these changes will be investigated to elucidate the mechanisms mediating the relationship between ncRNAs and cancer cell phenotypes that result from loss of pRB function. We hypothesize that some of the cellular changes that result from pRB loss are due to changes in ncRNA.

Results

Verifying Biological Significance and Trends of Misregulated Non-coding RNA

Symbol	Log2 Fold Change	P-value	Function
ASAP-IT1	1.794	3.53E-07	Involved in cell proliferation of lung cancer
KIRREL-AS2	1.777	1.57E-05	Adhesion of neurons and neuron defects
BDNF-AS	1.585	2.55E-12	Inhibitory effect on cell differentiation and migration
LOC340113	1.366	9.80E-05	Uncharacterized
N4BPL2-IT2	1.108	2.11E-05	Located near BRAC2; involved in breast cancer
LINC00342	1.06	3.79E-08	Upregulated in non-small lung cancer
PLCE-AS1	1.466	4.20E-04	Enhancer in gastric cancer
XIST	1.111	8.35E-04	Downregulated in breast cancer
CLSTN-AS1	1.399	4.31E-04	Pathological myopia

Table 1: Summary of misexpressed ncRNA and proposed function.

Previous literature has suggested the link between loss of pRB and misexpression of genes including non-coding RNAs (Nevins, 2001; Zhang et al., 2012; Dick & Rubin, 2013; Elchuri et al., 2018). Armed with this knowledge the results of the RNA screen (as seen in Figure 4) I first set to verify the biological upregulation of candidate ncRNA transcripts presented in Table 1 that had been implicated in cancer biology studied. I worked with non-transformed RPE-1 cells which were made to be pRB deficient via knockdown by a drug inducible short hairpin to disrupt pRB stability. This experiment was done in quadruplet, and each time 2 plates were prepared using the protocol above. Throughout each replicate, one of the plates was treated with 2ug/mL of Doxycycline for 48 hours to induce knockdown. Quantitative PCR analysis indicated that this approach was sufficient to reduce pRB protein levels to approximately 30% of that seen in control cells. With this degree of pRB depletion, I was unable to confirm upregulation of most

ncRNAs that were significantly upregulated in the RNAseq data set and found Kirrel-AS2 and

XIST to be significantly downregulated, which in contrast to the results of our RNAseq screen

A)
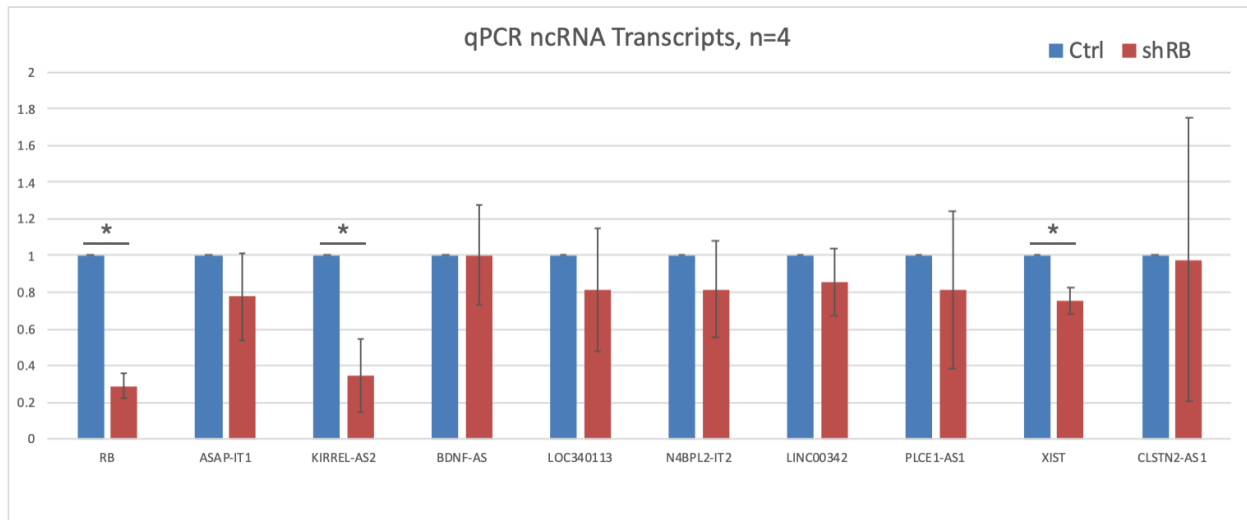
B)
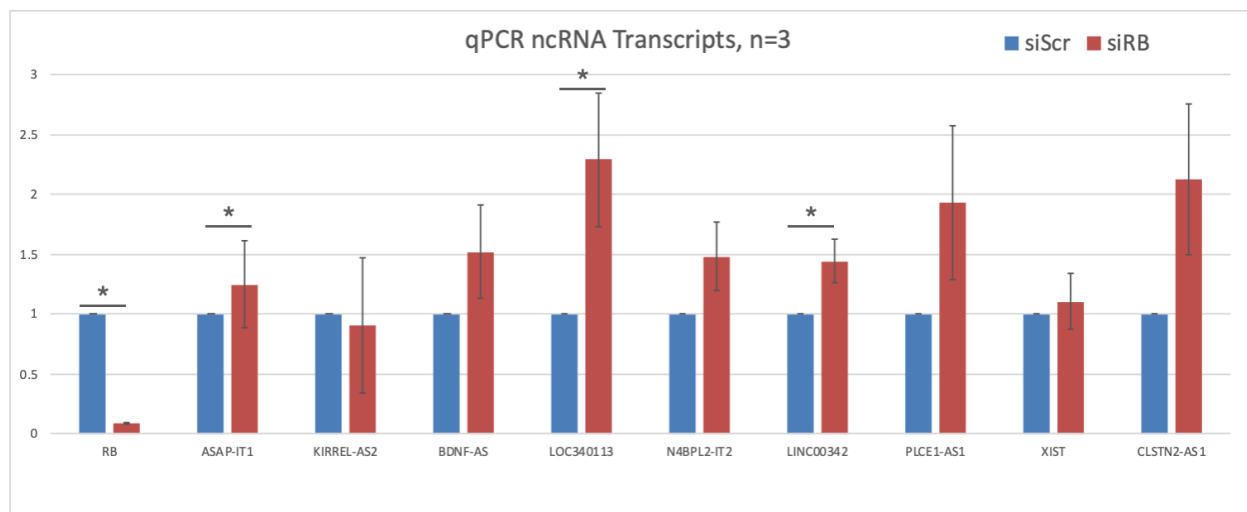
Figure 6: Loss of pRB causes altered expression of ncRNA. qPCR analysis of candidate ncRNA expression and compared to the control group, relative fold changes were presented as mean ± SD. **A)** Red represents shRB knockdown of pRB. Blue represents control cells. Kirrel-AS2 and XIST have significantly higher fold expression. **B)** Red represents siRNA knockout of pRB. Blue represents siScr which is our control. ASAP-IT1, LOC340113 and LINC00342 have significantly higher fold expression. (*) denotes P value < 0.05.

(Figure 4; Figure 6A). As a complementary approach I also assessed ncRNA levels in control

cells and those depleted of pRB using siRNA based depletion mechanisms. Consistent with the

RNAseq analysis (Figure 4), this approach resulted in a near complete depletion of pRB mRNA

(< x%) and led to the upregulation of several ncRNA transcripts, including ASAP-IT1,

LOC340113 and LINC00342 (Figure 6B).
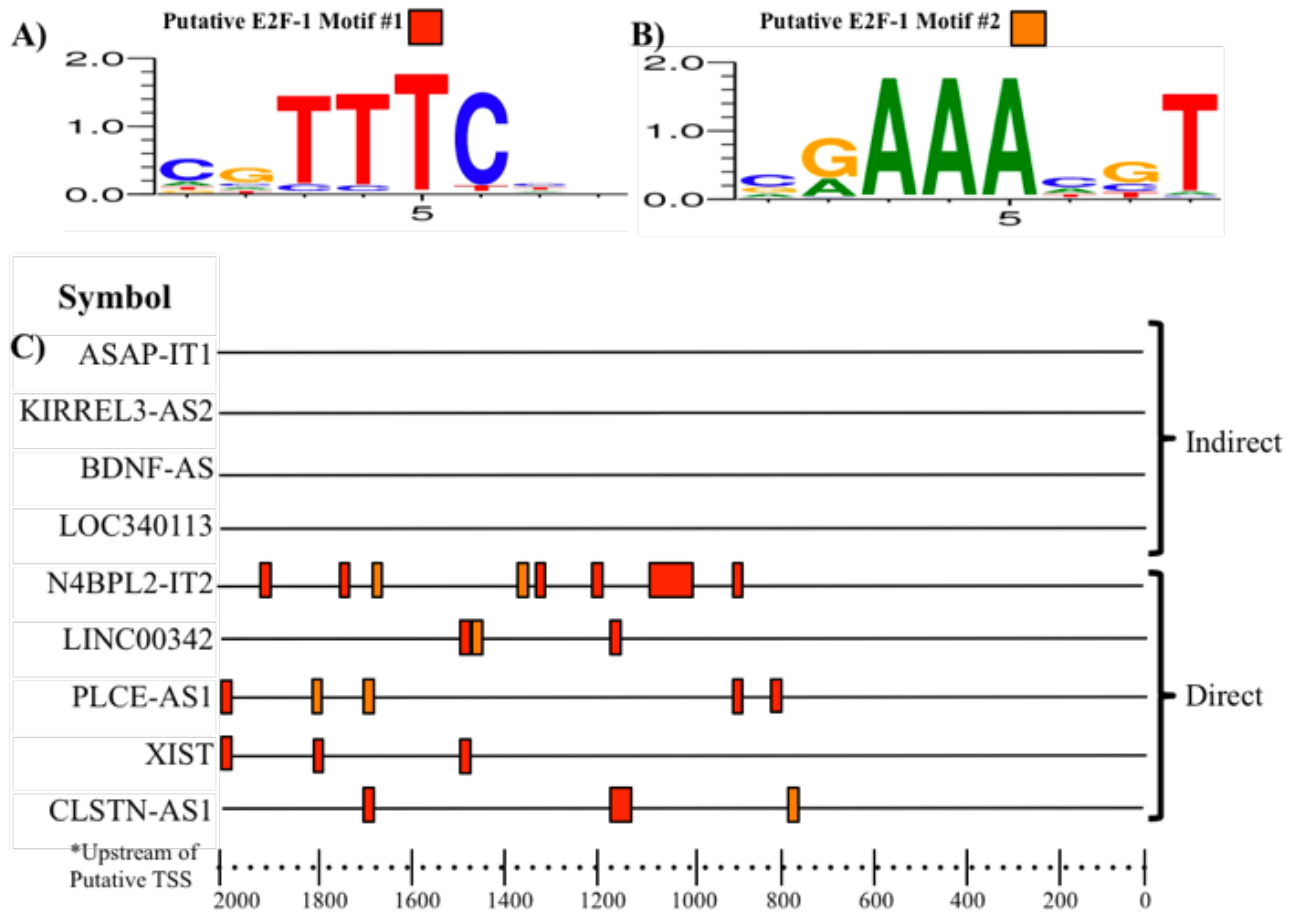
Figure 7: ncRNAs both lack and contain E2F-1 consensus sequences. The MotifMap: genome-wide maps
of regulatory elements tool was used to determine E2F's binding sequence logo. **A)** Motif #1 relates to a E2F
consensus sequence (HNTTTCHN) and **B)** Motif #2 corresponds to a E2F consensus binding sequence
(VRAAAHST). DTU Promoter 2.0 Prediction Server was used to predict transcription start sites (TSS) of the
ncRNA. Once the TSS was determined Broad Institute's Integrated Genomic Viewer Software's Motif Finder
tool was used. **C)** Hits generated from Motif Finder Tool once the consensus sequences (A) and (B) were
inputted.

Determining Putative E2F Binding Sequences on Candidate NcRNAs

In order to understand how these ncRNA's may be upregulated some initial work by the researchers Xue et al. (2007) was referred to. Their work provided hints of potential binding of E2F near the genomic loci of ncRNAs. The researchers proposed a potential transcriptional regulatory role of pRB and E2F on the expression of ncRNAs due to the output of their ChIP experiments (Xue et al., 2007). If pRB is compromised E2F is free to bind to genomic DNA and potentially upregulate and misexpress candidate ncRNAs for example (Nevin, 2001). Based on this idea, a number of free online tools and software were utilized to determine binding of E2F upstream of the transcription start site of the candidate ncRNA. Using sequences previously determined to be recognition sequences for E2F1 binding (Figure 7A and 7B), alignment software was used to determine potential E2F regulatory sequences on each ncRNA of interest. (Figure 7C). Potential E2F1 binding sites were identified upstream of five of the nine ncRNAs assessed (Figure 7C), suggesting that in some cases ncRNA upregulation following pRB loss represents direct regulation by E2F. The absence of E2F1 consensus sequence on other ncRNAs suggest pRB may also regulate ncRNA transcripts in an E2F1-independent manner.

Functional Outcomes of pRB Loss

To determine the functional relevance of loss of pRB-dependent ncRNA regulation, I explored the role of pRB in cell motility. Previous work had demonstrated the retinoblastoma cancer cells exhibit increased moitility Shang et al. (2018) but fell short of demonstrating that this change resulted from pRB loss and not from other changes in the cancer cells. Using movies generated by a previous student in the Manning lab, I sought to test the hypothesis that loss of pRB alone is sufficient to alter cell motility. Using an hTERT RPE-1 cell line that was

engineered to express an RFP-tagged histone 2B (H2B) to enable visualization of nuclei, cells were maintained at 37C and 5%CO2 while microscopic images were captured every 5 minutes for up to 36 hours. Using Cell Profiler software suite, I assessed the motility of control and pRB-depleted cells that were imaged as described above. A total of 100 cells that could be tracked for at least 12 frames or 1 hour were tracked in each condition were analyzed for their motility. I created a custom pipeline based on a template cell tracking pipeline produced by CellProfiler to assess the motility of the cells. This analysis made use of two powerful object processing modules: 1) 'IdentifyPrimaryObjects' and 2) 'TrackObjects'. Briefly, the RPE-1 control and siRB cells first had to be recognized by the software so that they could then be identified be identified and their xy coordinates determined for each time coordinate. From these xy coordinates, over time, cell velocity and total distance traveled could be calculated. These data aided in determining the displacement of these cells between frames using CellProfiler. Parameters used in optimizing these pipelines to efficiently identify and tract single cell nuclei can be found in the methods section.

First, I assessed cell motility of cells that were plated at low density and remained sub-confluent throughout the duration of the movie (<2.5h) (Figures 8A-C). When the average distance travelled by a single cell in a single frame (1 frame lasting 5 minutes) was assessed, pRB depleted RPE-1 cells were found to have a greater motility than control cells (Figure 8A). Additionally, when average displacement in the length of tracking was compared, siRB cells exhibited a significantly increased distance traveled than control cells (p<0.05; Figure 8B). Next, I assessed cell velocity and distance traveled of control and pRB-depleted in contact-inhibited populations of cells (imaged until confluency at 16.5-hour) (Figures D-F). As expected, control cells that experienced contact inhibition exhibited both decreased velocity and decreased

distance traveled. Interesting the pRB depleted RPE-1 cells maintain high motility as was seen in the assay performed at lower confluency.
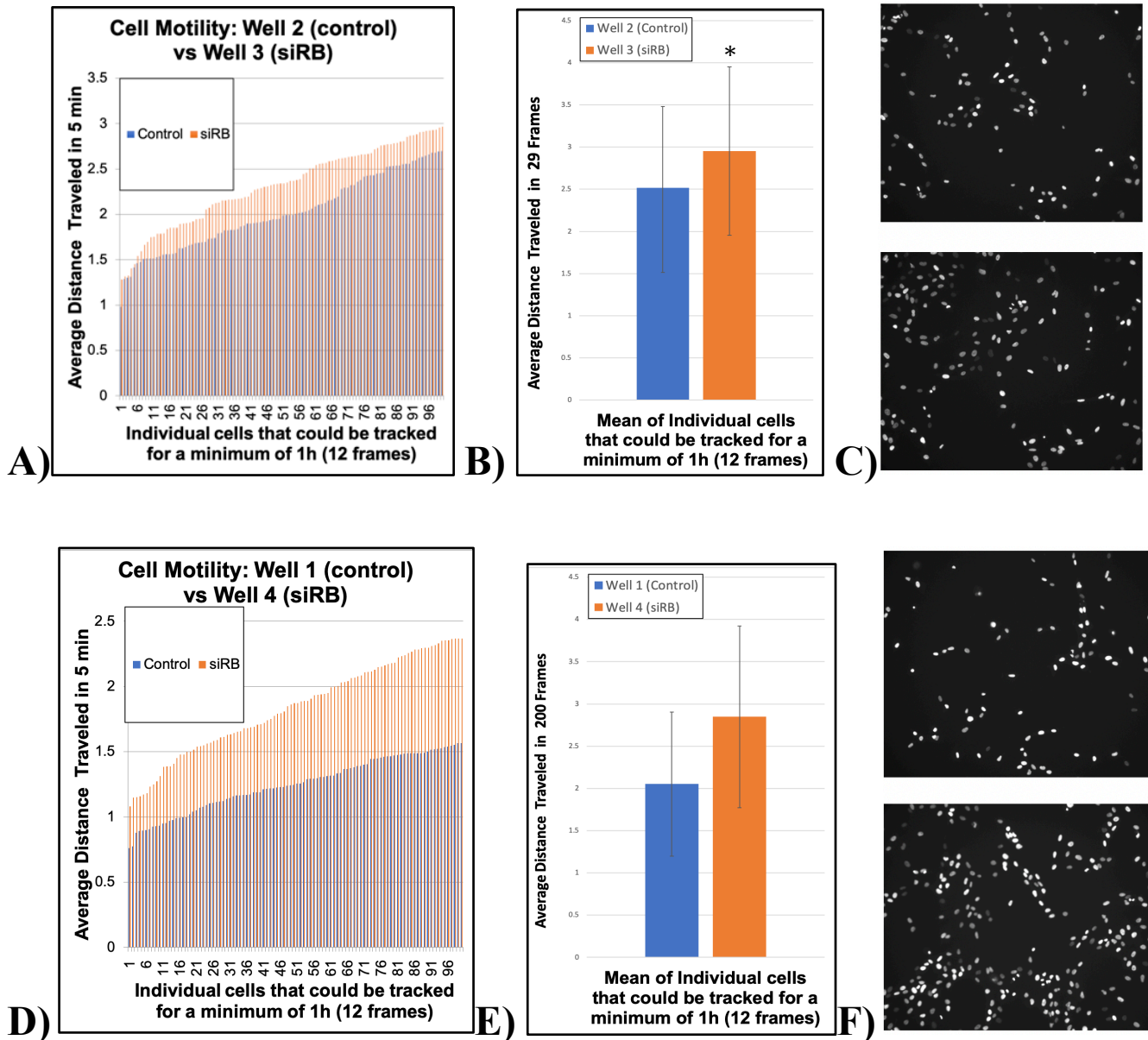
Figure 8: pRB deficient cells have altered motility. This experiment employed RPE-1 cells in which pRB was KO via siRNA, and control epithelial cells. Both of these cells were treated with a Histone 2 fluorescent label which aided in visualizing chromatin and nuclei of the cells. A) Distribution of low confluency wells 2 and 3, average distance traveled by individual cells in a 5 minute period or 1 frame, B) Average distance travelled in lifetime (29 frames) of all cells in a given well, C) Representative images of control epithelial cells at time minimum (frame 1; top) and maximum time point (frame 29; bottom). D) Distribution of high confluency wells 1 and 4, average distance traveled by individual cells in a 5 minute period or 1 frame, E) Average distance travelled in lifetime (200 frames) of all cells in a given well, F) Representative images of control epithelial cells at time minimum (frame 1; top) and maximum time point (frame 200; bottom).

Conclusions & Future Directions

Candidate NcRNAs May Be Regulated by Direct Binding of E2F

The data above highlights the downstream effects of pRB loss in terms of misexpression of candidate ncRNAs as well as phenotypic outcomes following knockout of pRB. One of the main aims of this project was to explore the role of the pRB-E2F complex as a potential transcriptional regulator of the candidate ncRNAs. Results have shown that ncRNAs both lack and contain putative E2F-1 binding sites (Figure 7). This is suggestive of direct regulation by the pRB pathway on the expression of ncRNA. Further experiments could be performed to verify the existence of these E2F-binding sites.

Common transcriptional gene expression reporter assays such as a luciferase reporter assay may be employed and have a proven efficacy in cell culture models (Barriscale et al., 2014). A luminescent reporter gene construct is prepared with the promoter region of interest cloned upstream of the luciferase gene; in this case it would include the regions where E2F-1 may directly bind in the promoter region of the ncRNA. The expression vector is than transfected in the cells and after an incubation period the cells are lysed to extract the luciferase enzyme, to which bioluminescent protein Luciferin is added in conjunction with other reagents (Barriscale et al., 2014). The luciferin is broken down by the luciferase enzyme, and this is then measured by specialized apparatus which can illustrate the activity of the promoter region (Barriscale et al., 2014). An ideal scenario for those candidate ncRNA that may be directly regulated E2F-1 binding sites may fluoresce initially, and then lose this fluorescence if these E2F binding sites are disrupted. This would be indicative of direct influence of the pRB pathway. It is also intriguing to consider the other ncRNA that lack E2F-1 consensus sequences, perhaps their expression may

be regulated by other members of the pRB-dependent interactions and this avenue must be further explored.

pRB Loss Promotes Misexpression of NcRNA

The data presented above affirms the notion that pRB loss is associated with the misexpression of candidate ncRNAs. Unfortunately, there was a discrepancy or rather a failure to produce consistent pRB knockdown via a shRB approach. This may explain why different candidate ncRNAs were significantly upregulated in the siRB qPCR analysis than compared to shRB knockdown of pRB. In both experiments, the majority of the ncRNAs were upregulated but not significantly, perhaps significance could have been reached by preparing and analyzing addition replicates. Another important consideration is that the altered expression of these candidate ncRNA may be sensitive to levels of pRB loss, with siRB producing a stronger depletion of pRB than shRB approaches.

Additionally, attempts were made to deduce whether or not the altered upregulation of ncRNAs may be specific to a specific phase of the cell cycle. These experiments made use of multiple cell synchronization approaches and DNA damaging reagents which were used to assess the sensitivity of ncRNA candidates to DNA damage, and to see at which point in the cell cycle these ncRNAs are misregulated following pRB loss. Further attempts could be made to explore ncRNA expression levels depending on the phase of the cell cycle. This may aid in devising future experiments, as different members of the pRB pathway are involved at different stages of the cell cycle.

pRB Deficient Cells Have Greater Motility Than Compared to Control Epithelial Cells

Alongside evidence for misexpression of candidate ncRNA, the potential implications of the upregulation were explored to further categorize the role of the candidate ncRNAs. Based on prior research, it appeared that one of the candidates BDNF-AS was implicated in having an inhibitory effect on cell proliferation and cell migration (Shang et al. (2018). This informed analysis of non-transformed RPE-1 cells in untreated control versus siRB knockdown of pRB conditions. Results from Figure 8 describe pRB depleted cells as having greater motility compared to control cells. These findings were consistent with what had been previously been described in tumor cell contexts, but our results were the first to demonstrate that pRB loss is sufficient to promote cell motility in a non-transformed human epithelial cell line. This altered motility could be verified by producing additional replicates or complementary assays. An intriguing experiment would be to attempt to deplete BDNF-AS to study the efficacy of this approach to reduce the motility of pRB deficient cells to levels seen in control cells.

Clinical Significance

pRB loss common in some human cancers is responsible for some of the hallmarks of cancer. When pRB is compromised many genes become dysregulated (as shown in Figure 4) which has many downstream effects on a cell, such as unregulated cell proliferation and altered motility and consequently flags numerous genes, as well as ncRNAs, that present different avenues for future therapies. One of the phenotypes explored was the motility of pRB deficient cells in non-transformed cells which is a novel approach. We posited that overexpression of certain ncRNAs could rescue the motility and restore it to control cells. The ncRNA we were interested in was BDNF-AS, which can be utilized as a dose-dependent novel therapeutic to treat pRB deficient cells. Most intriguing, however, is the evidence of the expression of ncRNAs may

be regulated by pRB-dependent mechanisms. Results showed that E2F-1 may bind directly to the

promoter region of some ncRNAs, perhaps further analysis of these consensus sequences may

provide future avenues for cancer therapeutics.

Methods

Identification of ncRNA Candidates

RNA sequencing data produced by the Manning lab in 2015 was used to determine ncRNAs of interest. RNAseq was performed on siRNA KO of RB in RPE-1 cells and multiple gene-specific libraries were employed which produced data of misexpressed genes. This dataset was imported to Excel 2015, and using the filter tool, the results were filtered to show ncRNAs that were misexpressed. Next, only those ncRNA with log2 fold change values of <-1 were sorted. A value of -1 means that in these siRNA treated cell lines, there is a 50% change in expression of a given gene than compared to an untreated cell line. Additionally, only those ncRNAs with p-value or significance of <0.001 were included in this initial analysis. This yielded a list of 10 ncRNA candidates.

Maintenance of Cell Culture

The adherent cell line human RPE-1 cells expressing a hTERT shRB were cultured in Dulbecco's Modified Eagle Medium (DMEM). This media contained 10% Fetal Bovine Serum (FBS) and 50ug/mL of streptomycin and penicillin.

This cell line was subcultured at a ratio of 1:5 after 48 hours, where the media was aspirated out and the plate was washed with 2mL of 1X PBS which was also aspirated. Next, 2 mL of trypsin was added to the cells and were left in an incubator for 5-6 minutes at 37◦C. After incubation, 8 mL of fresh DMEM+10%FBS media was added to the plate. The cell suspension was then moved to a new 15 mL conical tube and was centrifuged for 5 minutes at 1000 rpm to pellet the cells and remove trypsin from the cells. The media was then aspirated out and 10 mL of fresh media was used to resuspend the cells. 2mL of this cell suspension was removed from

the 15 mL conical tube to a new 10cm cell culture dish, and the total volume was increased to 10 mL with additional DMEM+10%FBS media.

Knockdown of pRB

This experiment was done in triplicates, and each time 2 plates were prepared using the protocol above. Throughout each replicate, one of the plates was treated with 2ug/mL of Doxycycline for 48 hours to induce knockdown at a ratio of 1:1000 of Doxycycline to total cell suspension volume.

RNA Extraction and Purification

Firstly the adherent human RPE-1 cells grown in a 10cm dish with a total volume of 10mL were homogenized at room temperature. The DMEM+10%FBS media was aspirated and 1mL of TRIzol reagent (Ambion) was added directly to the cells. The TRIzol aids in lysing the cells and lysis was ensured by pipetting up and down several times. Then approximately 1mL of lysed cells suspended in TRIzol were transferred to a 1.5mL eppendorf tube. Next a chloroform wash was performed to phase separate the sample. This step involved adding 0.2mL of chloroform was added and the tube was shaken vigorously for 15 seconds and was allowed to incubate at room temperature for 2 to 3 minutes. The sample was then centrifuged at 12000 x g for 15 minutes at 4◦C. After centrifugation the sample phase separates due to the addition of chloroform. The tube then contains a lower red phenol-chloroform organic phase which contains protein, and interphase that contains DNA and a clear upper aqueous phase which contains the RNA. 0.5mL of the upper aqueous phase, which holds approximately 50% of the total volume of

the sample, was transferred to a fresh tube. The chloroform wash was repeated on the contents of

fresh tube to extract to purify the RNA in the aqueous phase.

Next 0.5mL of 100% isopropanol was added to the tubes to precipitate the RNA. The

samples were incubated at room temperature for 10 minutes and then centrifuged at 12000 x g

for 10 minutes at 4°C. This step yields a gel like pellet at the bottom-side of the tube. The

supernatant was removed and the pellet was washed with 1mL of 75% ethanol. The tube was

then vortexed briefly and then centrifuged at 7500 x g for 5 minutes at 4°C. After centrifugation,

the supernatant was removed. This RNA wash step was repeated twice.

Next the pellet was allowed to air dry for 5-10 minutes. After this step the RNA was

resuspended in 25 µL of RNase free water. Finally the quality and quantity of the resuspend

RNA was assessed via a NanoDrop spectrophotometer (Thermofisher).

SYBR Green-based Quantitative real-time PCR (qrt-PCR) Protocol

RNA was extracted via TRIzol (Ambion) using the protocol above. Complementary

DNA was synthesized using 'High-Capacity cDNA Reverse Transcription Kit with RNase

Inhibitor' (Applied Biosystems). To assess, the knockdown of pRB and verify the expression

trends (generated from RNAseq analysis) of ncRNAs, quantitative real-time PCR was performed

using SYBR green kit (Applied Biosystems). qPCR was done on 96 well plates which included

GAPDH which acted as a control and gene specific primers for pRB and the ncRNA candidates.

The cycle threshold was normalized to the cycle threshold for GAPDH. Three biological

replicates were produced where each gene or ncRNA had two technical replicates within the

plate.

The following gene-specific primers were used:

Gene	Gene type	Forward Primer	Reverse Primer
ASAP1-IT1	ncRNA	TCCCTCCACAGAGTTTTGCC	ACCTCAGCTCCACGAAAACC
KIRREL3-AS2	ncRNA	GTTCAAGGATGGCAGCAGCAGG	CCCCCGTTCTTGATTGGAGT
BDNF-AS	ncRNA	TTCGGGAATGTGGCTAAGGG	CGGACCATCTGTTCTGCTGT
LOC340113	ncRNA	CGAGACCTTTGGACCAAGA	ATGCTGTCTCTCTGACGCTG
RAD21-AS1	ncRNA	CAAAATGGTACCTGTGCGCC	CTTTGCGCTTGCTCAGTTG
N4BP2L2-IT2	ncRNA	GCAAGCTTGATGAGGTCCCA	GACCAAGCAACAGTGAGCAA
LINC00342	ncRNA	CCACAGACTACCCAAAGCAG	TCACTCTGCTGCTTCAGAAAAT

PLCE1-AS1	ncRNA	CCCCTGATGTTTAACAC AACGTT	TGCTAACGTTCACCCAAG TT
CLSTN2-AS1	ncRNA	TGTTGCACAGGTCTCCT CAC	CCCCTGAGCCAACTCACT
XIST	ncRNA	GACACAAGGCCAACGA CCTA	TCGCTTGGGTCCTCTATCC A
RB	coding	TGGTGAATCATTCGGGA CTT	GGTTTAGGAGGGTTGCTT CC
GAPDH	coding	CCCTCTGGTGGCCCCTT	GGCGCCCAGACACCCAAT CC

Table 2: qPCR primer sequences.

Preparation of Input Protein Samples for Western Blotting

One additional replicate of the shRB KO was prepared so that protein could be extracted from it. These protein samples would aid in western blot procedures to confirm the knockdown of pRB.

First the adherent human RPE-1 cells grown in a 10cm dish with a total volume of 10mL had their media was aspirated. This plate was then washed with 3 mL of PBS which was then aspirated. Next, 2 mL of trypsin was added to the cells and were left in an incubator for 5-6 minutes at 37◦C. After incubation, 8 mL of fresh DMEM+10%FBS media was added to the plate. The cell suspension was then moved to a new 15 mL conical tube and was centrifuged for 5

28

minutes at 1000 rpm to pellet the cells and remove trypsin from the cells. The media was then aspirated out and 10 mL of fresh media was used to resuspend the cells.

Then 10µL of media was drawn from this 10mL conical. The 10µL was pipetted onto a hemocytometer which was used to count the cells. The volume to get 1×10^7 cells was determined and this volume of cells was added to a 1.5mL eppendorf tube. Next the sample in the eppendorf was resuspended in 3 times the calculated volume in 2X Laemmli buffer (Biorad). The 1.5mL eppendorf tubes were then transferred to a heat block set at 95°C for 2 minutes; the boiling ensured degradation of protein by denaturing proteases that may be present in the sample. Finally, these samples were stored at -20°C.

pRB Knockout via siRB

The siRNA knockout experiments were previously performed by members of the Manning lab. These knockout experiments were performed in triplicates but gene expression levels of candidate ncRNAs were not studied. To further verify the expression trends seen in the shRB knockdown and RNAseq analysis, previously stored RNA (at -80°C) was used to synthesize cDNA which was used to perform qPCR for the 10 ncRNA candidates in triplicate.

Cell synchronization and Knockdown of pRB Experimental setup

First the adherent human RPE-1 cells grown in a 10cm dish with a total volume of 10mL had their media was aspirated. This plate was then washed with 3 mL of PBS which was then aspirated. Next, 2 mL of trypsin was added to the cells and were left in an incubator for 5-6 minutes at 37oC. After incubation, 8 mL of fresh DMEM+10%FBS media was added to the plate. The cell suspension was then moved to a new 15 mL conical tube and was centrifuged for

5 minutes at 1000 rpm to pellet the cells and remove trypsin from the cells. The media was then aspirated out and 10 mL of fresh media was used to resuspend the cells. Then 10µL of media was drawn from this 10mL conical. The 10µL was pipetted onto a hemocytometer which was used to count the cells. A volume equivalent to 7.5×10^4 cells was plated on a 6 well dish and the total volume was increased with fresh DMEM+10%FBS media to 2mL.

Addition of small molecules

This experiment made use of the mitotic inhibiting drugs including Nocodazole (Sigma-Aldrich) at 100 ng/mL and Aphidicolin (Abcam) at 4µM. The DNA damaging reagent Hydroxyurea (Sigma-Aldrich) was used at 2mM. These reagents were resuspended in DMSO.

Three replicates were performed, each replicate of this experiment involved preparing two 6-well dishes where 4 wells of of the dish had 7.5×10^4 cells plated. One of the dishes had 2ug/mL of Doxycycline added to them to induce knockdown (at a ratio of 1:1000). The 2 plates were allowed to grow for 48 hours. After 48 hours the plates were treated with small molecules except for the control well, and were kept in drug for 16 hours. It is important to note that each plate included wells for: a control (no addition of small molecule), Nocodazole, Aphidicolin and Hydroxyurea.

RNA Extraction, cDNA Synthesis and qPCR from 6 well dish

After a 16 hours, RNA was extracted from the 6 well plates. Firstly the adherent human RPE-1 cells grown in the 6 well dishes with a total volume of 2mL per well were homogenized at room temperature. Then the DMEM+10%FBS media was aspirated from the dish. A PBS wash was performed and the added PBS was aspirated as well. Next, 250uL of TRIzol (ambion)

reagent directly to the cells to collect. Then approximately ~250uL of lysed cells suspended in TRIzol was transferred to a 1.5mL eppendorf tube. Next a chloroform wash to phase separate the sample was performed. This step involves adding 50uL of chloroform to the tube which is to be shaken vigorously for 15 seconds and was allowed to incubate at room temperature for 2 to 3 minutes. The samples were then centrifuged at 12000 x g for 15 minutes at 4°C. After centrifugation the sample phase separates due to the addition of chloroform. ~125uL of the upper aqueous phase should be transferred to a fresh tube. The chloroform wash was repeated once more, but with 2µL of chloroform. Then transfer ~125µL of aqueous phase to fresh tubes. After this step, 0.5uL of glycol blue was added to aid in visualizing pelleted RNA at later steps. Next, 100% isopropanol was added to the tubes, at a volume 5 fold of what the volume of the aquesous phase that was collected. The samples were incubated Isopropanol and glycol blue at room temperature for 10 minutes and then centrifuged at 12000 x g for 10 minutes at 4°C. A pellet was visualized and the supernatant was removed. An ethanol wash with 1mL of 75% ethanol and centrifugation at 7500 x g for 5 minutes at 4°C was performed. After centrifugation the supernatant was removed, and the ethanol wash was repeated once more. Once the supernatant was removed, the pelleted RNA was air dried for 5-10 minutes. Finally the pellet was resuspended in 20 µL of RNase free water and the quality and yield were assessed via the NanoDrop spectrophotometer (Thermofisher).cDNA and qPCR was performed in accordance with 'SYBR Green-based Quantitative real-time PCR (qrt-PCR) Protocol.'

Determining Putative E2F Binding Sites

      E2F consensus sequences were extracted from by the University of California, Irvine's free online tool called MotifMap. This database contains a comprehensive genome-wide map of

regulatory elements which includes transcription factor consensus sequences. Out of 21 entries only 2 were enriched in the promoter region of the candidate ncRNAs; HNTTTCHN (Human, E2F-1 consensus sequence) and VRAAAHST (Human, E2F-1 consensus sequence). In order to align these E2F-1 consensus sequence in the promoter region of ncRNA, two different promoter region servers were used to determine the transcriptional start sites (TSS). The first tool used was University of California Santa Cruz's genome browser tool. The candidate ncRNA were searched for, and the genomic DNA sequence was extracted. This website also has a variety of checkboxes so that only the annotated promoter region can be exported. In order to confirm the TSS and promoter region, the whole genomic DNA sequence was inputted in the Technical University of Denmark's online promoter prediction server. This powerful tool leverages complex algorithms to simulate binding of transcription factor interactions in the promoter region of the inputted sequence and gives a statistical prediction of a likely TSS. Once the TSS was determined the Broad Institute's Integrative Genomics Viewer software was used to align the consensus sequences in the promoter region of the ncRNAs. Specifically, the motif finder tool was used, where the consensus sequences were inputted to generate hits illustrated in Figure 7.

Cell Motility Assay

This experiment involved analyzing the 2-dimensional motility of control and pRB deficient cells using movies that were generated by a previous student in the Manning Lab. The previous student made use of an hTERT RPE-1 cell line. This cell line was constructed so that it was able to express red fluorescent protein tagging histone 2B (RFP-H2B). This allowed for the nuclei to be visualized which aided in the analysis of the cells using the Cell Profiler software

suite. The previous student maintained and subcultured the cells using a similar protocol as noted above. Microscopic images were collected every 5 minutes for up to 36 hours.

In order to track the motility of the cells, the Cell Profiler Software parameters had to be optimized to track the cells properly. Firstly, I downloaded a default 'Object Tracking and Metadata Management' pipeline. This pipeline or series of functions was set up to track multiple objects (cells in this case) and several sequences of images in a time-lapse experiment and is optimized to track moving cells from frame to frame, which is a challenging task. The first step was to drag and drop this pipeline onto the sotware which then automatically loads the various functions in the pipeline. Next the images are dragged and dropped into the software. It is at this point that a naming convention must be established, so that the software is able to extract the metadata of the images including: 1) the well ID, 2) frame number and 3) timepoint or frame number. Cell Profiler is capable of extracting the metadata automatically (Figure 9), but sometimes the software is unable to detect it thus the formula: ^(?P<Well>.*)_ (?P<Treatment>.*)_ 1T(?P<timepoint>[0-9]*) must be used. To further breakdown this formula, the function '?P' tells the software to begin to search the title for or string which is enclosed in '< >.' Finally we must inform the software of what the numeric range is which is denoted by giving a range of values enclose in '[].'
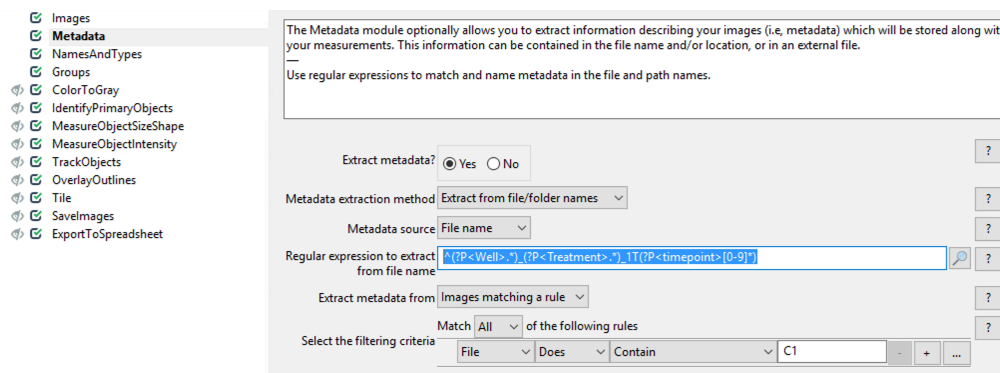
Figure 9: Screenshot of cell profiler software metadata tab.
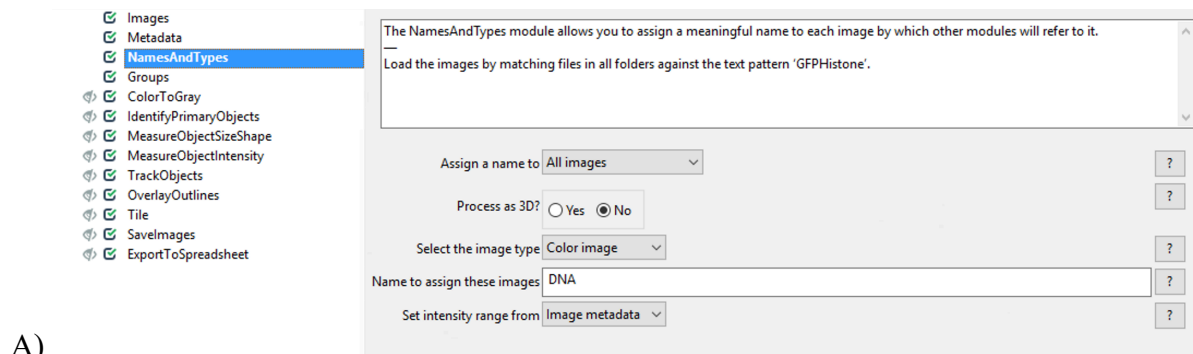
A)
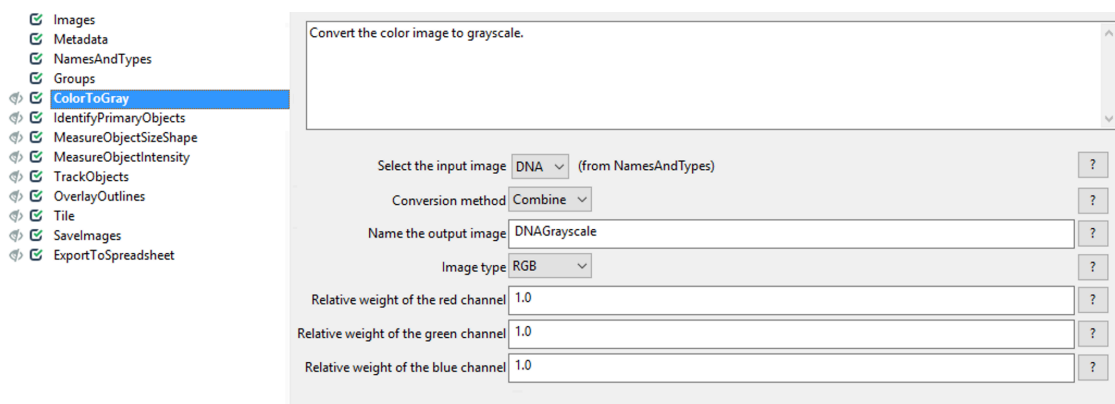
B)

Figure 10: Screenshot of cell profiler software. A) NamesAndTypes module and B) Color to Gray module.

Subsequently, the software must be told what to label the images for analysis (Figure 10A), since this analysis is looking at nuclei of cells the name assigned was 'DNA.' This is important as we need to refer to these batch of images in order to convert them to grayscale, which is essential when assessing the morphology of cells as grayscale allows for just accounting for intensity of signal rather than intensity of a colored channel for example. Figure 10B shows the settings used, The output images were called 'DNAGrayScale.'

Identify the fly embryos from the histone stain image. Three-class thresholding works better than the default two-class method.

- Images
- Metadata
- NamesAndTypes
- Groups
- ColorToGray
- **IdentifyPrimaryObjects**
- MeasureObjectSizeShape
- MeasureObjectIntensity
- TrackObjects
- OverlayOutlines
- Tile
- SaveImages
- ExportToSpreadsheet

Use advanced settings?	⦿ Yes ◯ No
Select the input image	DNAGrayscale ∨ (from ColorToGray #05)
Name the primary objects to be identified	Cells
Typical diameter of objects, in pixel units (Min,Max)	20 30
Discard objects outside the diameter range?	⦿ Yes ◯ No
Discard objects touching the border of the image?	⦿ Yes ◯ No
Threshold strategy	Global ∨
Thresholding method	Otsu ∨
Two-class or three-class thresholding?	Three classes ∨
Assign pixels in the middle intensity class to the foreground or the background?	Background ∨
Threshold smoothing scale	1.3
Threshold correction factor	1.0
Lower and upper bounds on threshold	0.02 1.0
Method to distinguish clumped objects	Shape ∨
Method to draw dividing lines between clumped objects	Intensity ∨
Automatically calculate size of smoothing filter for declumping?	⦿ Yes ◯ No
Automatically calculate minimum allowed distance between local maxima?	⦿ Yes ◯ No
Speed up by using lower-resolution image to find local maxima?	⦿ Yes ◯ No

View output settings
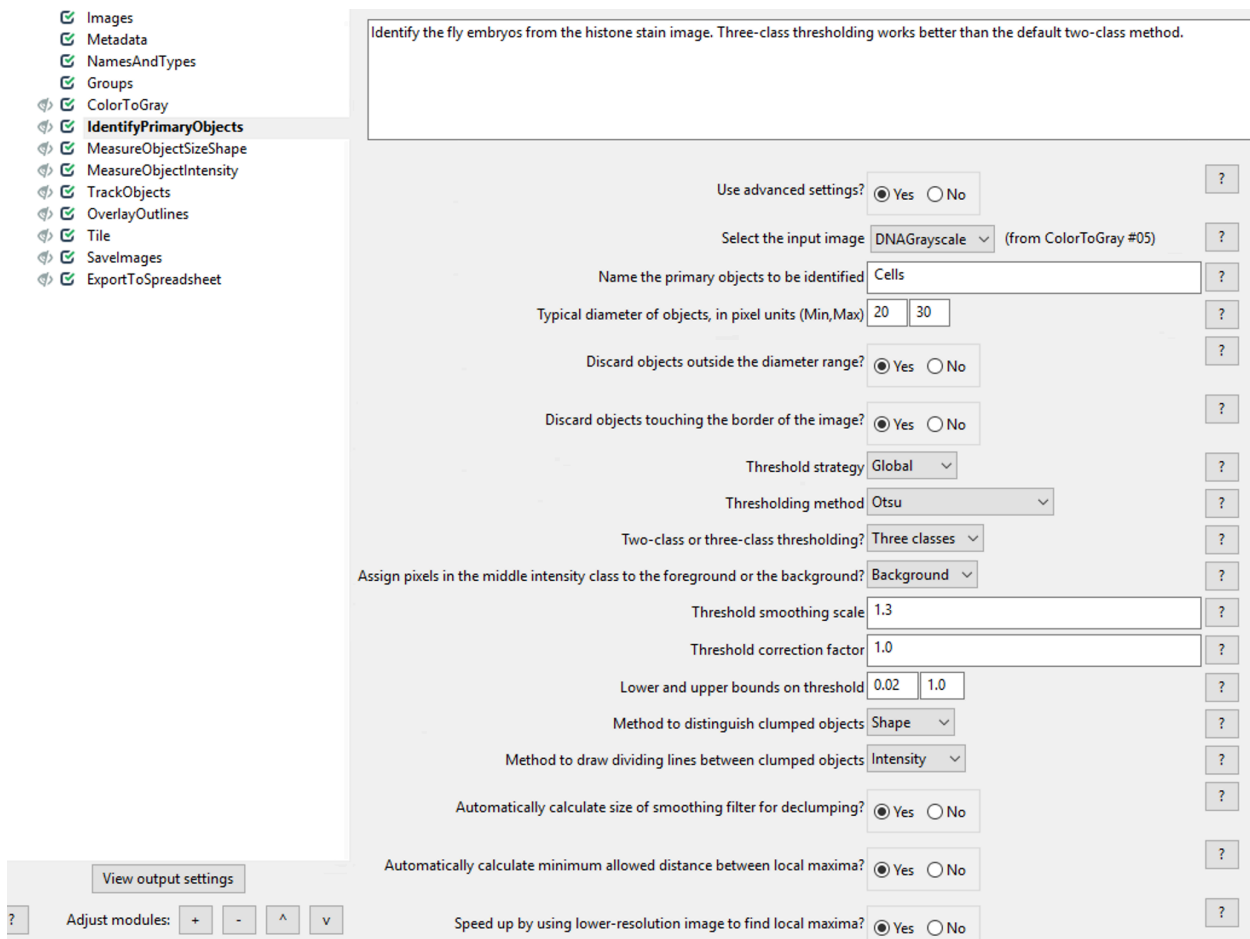
? Adjust modules: + - ^ v

Figure 11: Screenshot of Cell Profiler Software IdentifyPrimaryObjects module.

Unfortunately, the default pipeline was having trouble tracking all the cells in a frame of view due to differential fluorescent intensity. Thus, the parameters were adjusted as seen in Figure 11. The most important variable to adjust was threshold smoothing scale as well as correction factor. These values could be the difference from the software perceiving two cells close to each other as one or 2 distinct cells. The thresholding method was also important; this analysis made use of the Otsu method which involves producing a histogram of the spread of the intensity of individual pixels of the cell and is able to more distinctly tell two cells apart as this algorithm is able to reduce the signal of the intensity in ways that are beyond the scope of this project (Dongju Liu, 2009). The software also had to be instructed as two what is a typical range of

diameter of the cells. This was a rudimentary task, as the raw images were opened in the

software and using the ruler function the diameter was measured for around 10 cells to

appreciate the range of diameters of cells. The measurements made by this module include a

count of the objects tracked as well as the xy coordinates of each of the identified cells.
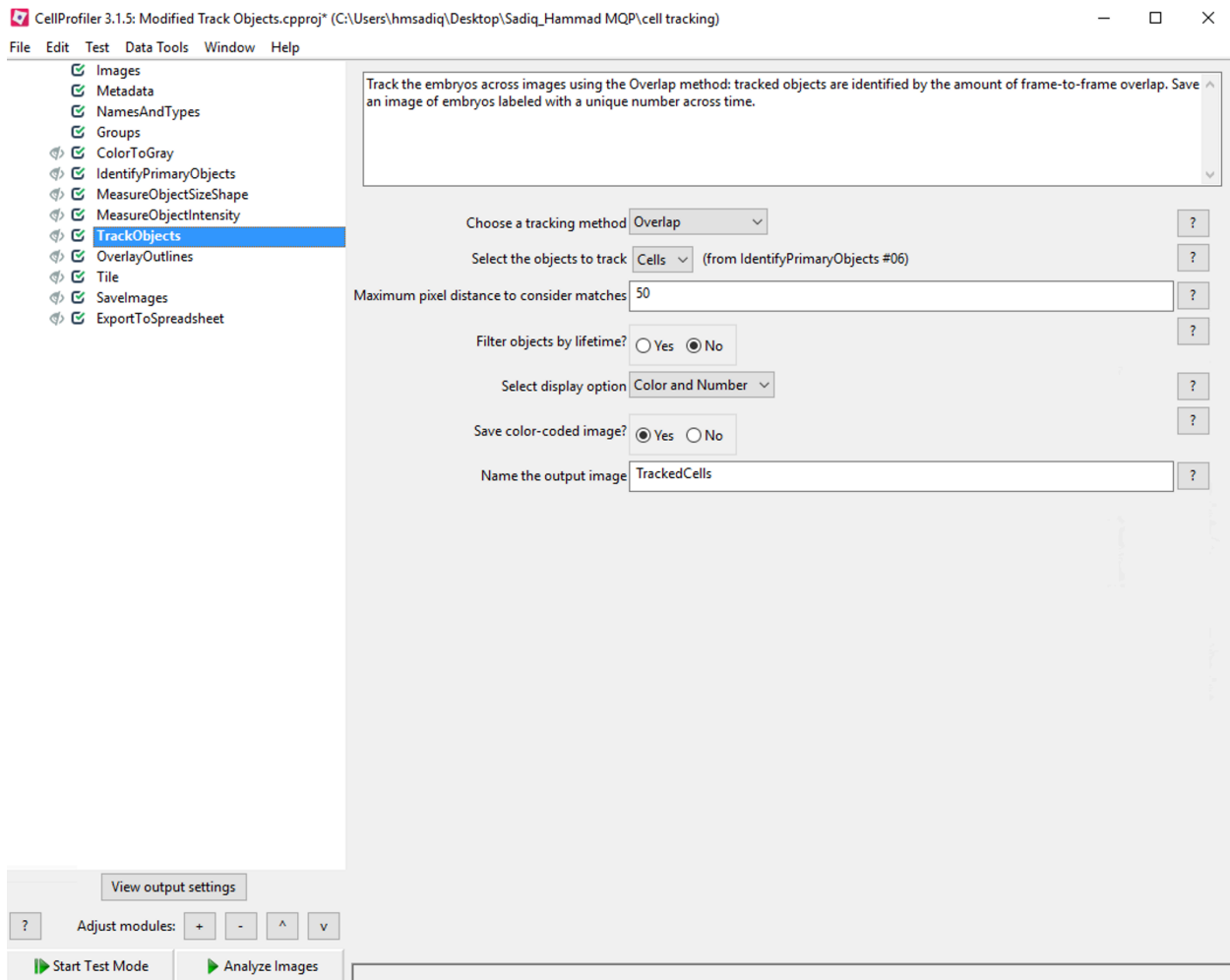

Figure 12: Screenshot of Cell Profiler Software TrackObjects module.

This function was instrumental in the analysis of the motility of the cell. The module

outputted the displacement which is the shortest distance traveled by the object between two

points. Perhaps most importantly, this module kept track of the labeled objects. This is an

important point which complicated the motility analysis. The module from Figure 11 outputs the

number of objects tracked, but for example, if a cell leaves the field of view and comes back, it is perceived as a new object. This is in contrast to the label output which uniquely identifies a cell in the lifetime of the movie. For our analysis we looked at a totally of 100 cells that were labeled and could be tracked for a minimum of 12 frames or an hour.

References

- Nevins, J.R. "The Rb/E2F Pathway and Cancer." *Human Molecular Genetics*, vol. 10, no. 7, 2001, pp. 699–703, doi:10.1093/hmg/10.7.699.

- Cavenee, W.K., Dryja, T.P., Phillips, R.A., Benedict, W.F., Godbout, R., Gallie, B.L., Murphree, A.L., Strong, L.C. and White, R.L. (1983) Expression of recessive alleles by chromosomal mechanisms in retinoblastoma. Nature , 305, 779–784.

- Dyson, N.J. (2016). Rb1: a prototype tumor suppressor and an enigma. Genes Dev 30:1492-1502

- Knudsen, Erik S., and Karen E. Knudsen. "Tailoring to RB: tumour suppressor status and therapeutic response." Nature Reviews Cancer, vol. 8, no. 9, 2008, p. 714+. Health Reference Center Academic. Accessed 27 Feb. 2018.

- Frederick A. Dick, & Seth M. Rubin. (2013). Molecular mechanisms underlying RB protein function. Nature Reviews Molecular Cell Biology, 14(5), 297–306. https://doi.org/10.1038/nrm3567

- Peurala, E., Koivunen, P., Haapasaari, K., Bloigu, R., & Jukkola-Vuorinen, A. (2013). The prognostic significance and value of cyclin D1, CDK4 and p16 in human breast cancer. Breast Cancer Research : BCR, 15(1), R5–R5. https://doi.org/10.1186/bcr3376

- Weinberg, R. (1995). The retinoblastoma protein and cell cycle control. Cell, 81(3), 323–330. https://doi.org/10.1016/0092-8674(95)90385-2

- Horowitz, J. M., Park, S.-H., Bogenmann, E., Cheng, J.-C., Yandell, D. W., Kaye, F. J., Minna, J. D., Dryja, T. P., and Weinberg, R. A. (1990). Frequent inactivation of the retinoblastoma antioncogene is restricted to a subset of human tumor cells. Proc. Natl. Acad. Sci. USA 87, 2775-2779.

- Tong, J., Sun, X., Cheng, H., Zhao, D., Ma, J., Zhen, Q., … Bai, J. (2011). Expression of p16 in non-small cell lung cancer and its prognostic significance: A meta-analysis of published literatures. Lung Cancer, 74(2), 155–163.

- Elchuri, S., Rajasekaran, S., & Miles, W. (2018). RNA-Sequencing of Primary Retinoblastoma Tumors Provides New Insights and Challenges Into Tumor Development. Frontiers in Genetics, 9. https://doi.org/10.3389/fgene.2018.00170

- Zhang J, Benavente CA, McEvoy J, Flores-Otero J, Ding L, Chen X, Ulyanov A, Wu G, Wilson M, Wang J, Brennan R, Rusch M, Manning AL, Ma J, Easton J, Shurtleff S, Mullighan C, Pounds S, Mukatira S, Gupta P, Neale G, Zhao D, Lu C, Fulton RS, Fulton LL, Hong X, Dooling DJ, Ochoa K, Naeve C, Dyson NJ, Mardis ER, Bahrami A, Ellison D, Wilson RK, Downing JR, Dyer M. Nature. 2012 Jan 11; 481(7381):329-34.

- Xu X. Q., Bieda M., Jin V. X., Rabinovich A., Oberley M. J., Green R., et al. (2007). A comprehensive ChIP-chip analysis of E2F1, E2F4, and E2F6 in normal and tumor cells reveals interchangeable roles of E2F family members. 17 1550–1561. 10.1101/gr.6783507

- Kruer, Traci L., et al. "Expression of the lncRNA Maternally Expressed Gene 3 (MEG3) Contributes to the Control of Lung Cancer Cell Proliferation by the Rb Pathway." Plos One, vol. 11, no. 11, 2016, pp. E0166363.

- Huarte, M. (n.d.) (2015). The emerging role of IncRNAs in cancer. Nature Medicine, 21(11), 1253–1261. https://doi.org/10.1038/nm.3981

- Schmitt, Adam M., and Howard Y. Chang (2016). "Long Noncoding RNAs in Cancer Pathways." Cancer cell 29.4 (2016): 452–463. PMC. Web. 13 Oct. 2018.

- Romano, G et al. (2017) "Small Non-Coding RNA and Cancer." Carcinogenesis 38.5 485–491. Web.

- Wang, M., Ma, X., Zhu, C., Guo, L., Li, Q., Liu, M., & Zhang, J. (2016). The prognostic value of long non coding RNAs in non small cell lung cancer: A meta-analysis. Oncotarget, 7(49), 81292–81304. https://doi.org/10.18632/oncotarget.13223

- Zhuang, M., Gao, W., Xu, J., Wang, P., & Shu, Y. (2014). The long non-coding RNA H19-derived miR-675 modulates human gastric cancer cell proliferation by targeting tumor suppressor RUNX1. Biochemical and Biophysical Research Communications, 448(3), 315–322. https://doi.org/10.1016/j.bbrc.2013.12.126

- Tang, H., Zhao, L., Li, M., Li, T., & Hao, Y. (2019). Investigation of LINC00342 as a poor prognostic biomarker for human patients with non-small cell lung cancer. Journal of Cellular Biochemistry, 120(4), 5055–5061. https://doi.org/10.1002/jcb.27782

- de Farias, C., Heinen, T., Dos Santos, R., Abujamra, A., Schwartsmann, G., & Roesler, R. (2012). BDNF/TrkB signaling protects HT-29 human colon cancer cells from EGFR inhibition. Biochemical and Biophysical Research Communications, 425(2), 328–332. https://doi.org/10.1016/j.bbrc.2012.07.091

- Shang, W., Yang, Y., Zhang, J., & Wu, Q. (2018). Long noncoding RNA BDNF-AS is a potential biomarker and regulates cancer development in human retinoblastoma. Biochemical and Biophysical Research Communications, 497(4), 1142–1148. https://doi.org/10.1016/j.bbrc.2017.01.134

- Barriscale, K., O'sullivan, S., & Mccarthy, T. (2014). A single secreted luciferase-based gene reporter assaySingle luciferase reporter assay. Analytical Biochemistry, 453(1), 44–49. https://doi.org/10.1016/j.ab.2014.02.019

- Dongju Liu, & Jian Yu. (2009). Otsu Method and K-means. In 2009 Ninth International Conference on Hybrid Intelligent Systems (Vol. 1, pp. 344–349). IEEE. https://doi.org/10.1109/HIS.2009.74